Frontiers of Information Technology & Electronic Engineering
www.jzus.zju.edu.cn; engineering.cae.cn; www.springerlink.com
ISSN 2095-9184 (print); ISSN 2095-9230 (online)
E-mail: jzus@zju.edu.cn

Grazing incidence polarized light imaging of footwear prints*

Xin-yi BI[1,2], Rui-fang HAN[1,3], Ran LIAO[†‡1,4], Wu-sheng FENG[5], Da LI[1,3], Xue-jie ZHANG[5], Hui MA[1,3,6]

[1]*Shenzhen Key Laboratory for Minimal Invasive Medical Technologies, Graduate School at Shenzhen, Tsinghua University, Shenzhen 518055, China*

[2]*Department of Biomedical Engineering, Tsinghua University, Beijing 100084, China*

[3]*Department of Physics, Tsinghua University, Beijing 100084, China*

[4]*Division of Ocean Science and Technology, Graduate School at Shenzhen, Tsinghua University, Shenzhen 518055, China*

[5]*Criminal Police Team, Municipal Public Security Bureau, Zhuhai 519000, China*

[6]*Tsinghua-Berkeley Shenzhen Institute, Shenzhen 518071, China*

[†]E-mail: liao.ran@sz.tsinghua.edu.cn

Received June 21, 2018; Revision accepted Oct. 18, 2018; Crosschecked Nov. 12, 2019

Abstract: Footwear prints are important evidence in criminal investigation. They represent changes in the surface morphology due to disturbance to fine particle distributions. Existing non-contact optical detection methods usually measure the light intensity contrasts between the footwear prints and the ground, which can be enhanced by grazing incident illumination. We take polarization images of footwear prints on different types of floors using a commercial single lens reflex color camera. Results show that adding linear polarizers in front of the camera lens and light source improves the contrast of footwear print images. The best contrasts are achieved in degree of linear polarization. In addition, the three-color channels of the camera can be used to examine the spectral features of the polarization images. According to the experimental results, the best contrast is obtained at the blue channel. The current work shows that grazing incidence polarized light imaging can effectively enhance the contrast of the footwear prints against the floors, which would help obtain footwear evidence in criminal investigation.

Key words: Polarization; Image enhancement; Scattering; Particle
https://doi.org/10.1631/FITEE.1800383 **CLC number:** TP391

1 Introduction

When crime has been committed or initiated, many important indications are left by criminals, such as fingerprints, bloods, hairs, and footwear prints. These clues play a significant role in investigation of the crime scenes. Fingerprints and DNA have been frequently used to identify the crime and criminals. However, footwear prints can provide valuable forensic evidence as well (Wagle, 2015). They reflect not only the trails of criminals, but also plenty of personal information, such as height, weight, sex, and walking habits (Nakajima et al., 2000; Krishan, 2007; Li ZW et al., 2011). Criminal investigators can infer the personal characteristics of criminals by extracting and analyzing the footwear prints in the crime scene (Shaler, 2011).

Among the variety of methods to extract footwear prints (Herod and Menzel, 1982; Mora and Sbarbaro, 2005; Bennett et al., 2009; Sheets et al., 2013), optical methods have attracted more and more attention since they are non-contact and non-destructive methods. However, optical images of

‡ Corresponding author

* Project supported by the National Natural Science Foundation of China (Nos. 41527901 and 61527826), the Science and Technology Project of Shenzhen, China (Nos. SGLH20150216144502856 and JCYJ20160818143050110), the Chinese Academy of Sciences (No. XDB06020203), and the Open Grant of Key Lab of Trace Science and Technology, Ministry of Public Security, China (No. 2014FMKFKT06)

ORCID: Xin-yi BI, http://orcid.org/0000-0001-8315-3712; Ran LIAO, http://orcid.org/0000-0002-3088-2230

footwear prints can be seriously influenced by the surface conditions of the object, leading to ambiguity in details of the footwear prints. Using grazing incidence illumination and taking pictures right above the samples to collect scattered light at the vertical direction, one can effectively reduce the interference due to background reflection and enhance the contrast of the images (Renaud et al., 2009).

It has been known that for polarized photon scattering, polarization states of the scattered light are sensitive to the microstructure of the samples (Webster, 1998; Wang et al., 2016). In polarization modulation optics, such as polarizers and waveplates, the direction of a light beam is not altered, so it is a relatively simple task to upgrade an ordinary non-polarization optical system to a polarized version by inserting polarization optical components into the existing optical path. There have been more and more applications of polarization measurement in different fields, such as marine algae probing, atmospheric remote sensing, and bioinstrumentation (Tyo et al., 2006; Namer et al., 2009; Ghosh and Vitkin, 2011; Snik et al., 2014; York et al., 2014; Tuchin, 2016; Li et al., 2018; Wang et al., 2018). Polarized light imaging has been used to detect and enhance footwear impression (Bodziak, 1999).

When grazing incident light illuminates the particles, both intensity and polarization states of the scattered light are closely related to the size, shape, and composition of the particles (Zinov'eva, 2008; Svensen et al., 2011; Liou et al., 2013). Due to the difference of the scattering parameters between the footwear print and the background surface, the polarization states of the scattered light are usually different. By polarization detection, the footwear print and the object surface can be distinguished effectively, thereby improving the quality of footwear print images.

However, for many types of floor surfaces in household and public places, footwear prints usually do not show up clearly. The roughness parameter of these surfaces is at the micron level (Li KW et al., 2011), so the scattering is somehow sensitive to the wavelength of the light (Bohren and Huffman, 1983). In this case, a system that combines grazing incidence, polarization, and color may serve as an extra contrast mechanism to differentiate scattered light by particles of different sizes and to enhance the footwear print images.

With the rapid improvements in the technical specifications and cost efficiency of consumer-grade electronics, single lens reflex (SLR) color digital cameras become much cheap and easily available (Shin et al., 2010). As they are battery powered, completely portable, and of low cost, more and more researchers have used them as components of experimental systems (Migliavacca et al., 2011; Anderson and Gaston, 2013; Cai et al., 2017).

In this study, we combine the grazing incidence footwear print detection method, linear polarization illumination and detection, and an SLR color camera to improve the contrast of images. We place linear polarizers in front of both the illumination lamp and the camera (Wolff, 1997), and examine in detail how contrasts of the footwear print images are affected by different polarizations. We also carry out Monte Carlo simulations (Yun et al., 2009; del Moral, 2013) of polarized photon scattering on spherical scatters to explain the contrast mechanism in such measurements.

2 Experimental setup

Experimental setup for the polarized grazing incidence footwear print measurements is shown in Fig. 1. The illumination light source is the wide-field footwear print search light (Model FGZJD, Shengxin Electronic Technology Co., Ltd., China). The light source provides high brightness illumination by a line of LEDs with a total power of 150 W and a total light intensity of not less than 3500 lx at color temperature 6000 K. The light source is designed to search over a wide range of areas for extracting footwear prints or other fibrous trace material evidence. When placed on the ground, LEDs illuminate the ground at an incident angle of 80° to 90° through the rectangular side window of the light source. If the camera is placed directly above the potential footwear print, such a lighting method can effectively suppress most of the reflected light from the ground and bring up the contrast of footwear print images (Fig. 1).

In this work, most footwear prints are left on the polyvinyl chloride (PVC) floor cover, which is commonly used in many household or public settings, such as living rooms, porches, public halls, and corridors. Dusts and footwear prints on such types of surfaces do not show up clearly, making it difficult to

observe footwear prints on these surfaces by naked eyes or ordinary photography under ordinary unpolarized light sources. For comparison, we prepare similar footwear prints on two types of household tiles bought from a nearby store (Figs. 1c and 1d). The tiles are made of ceramic materials with rough surfaces for anti-slippery purpose.

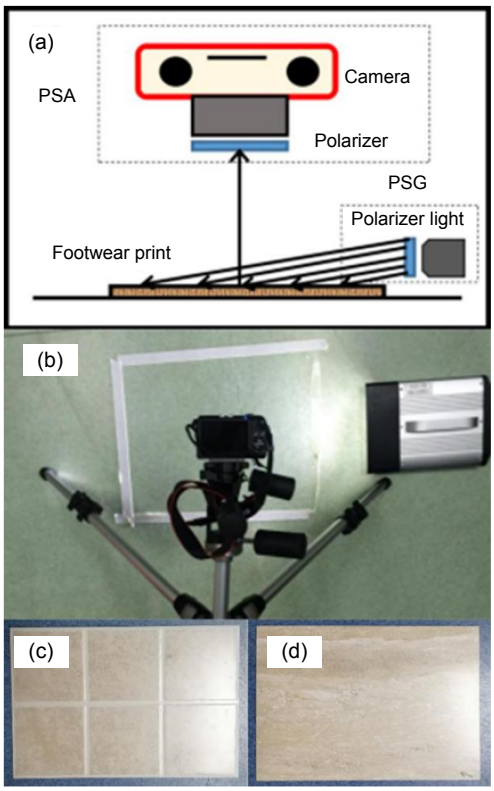

Fig. 1 Scene design of the experimental system: (a) schematic of the experimental setup; (b) real scene; (c) tile 1 bearing footprints; (d) tile 2 bearing footprints

Images are taken by a commercial SLR color camera (Canon EOS M2, 22.3 mm×14.9 mm, 3456×5184 pixels, 16-bit CMOS). In all the experiments, the camera is placed about 40 cm directly above the illuminated area by the wide-field footwear print search light. The ISO setting of the camera is 100. The exposure value is set to 250 μs.

The above experimental setup is easily modified for polarization imaging. A plastic polarizer sheet (thorlabs) can be placed in front of the light source window as the linear polarization state generator (PSG). An ordinary polarizer filter matching the Canon EOS M2 camera lens is used as the linear polarization state analyzer (PSA), which can be rotated easily without disturbing the camera focus for taking different linear polarization components (Fig. 2).

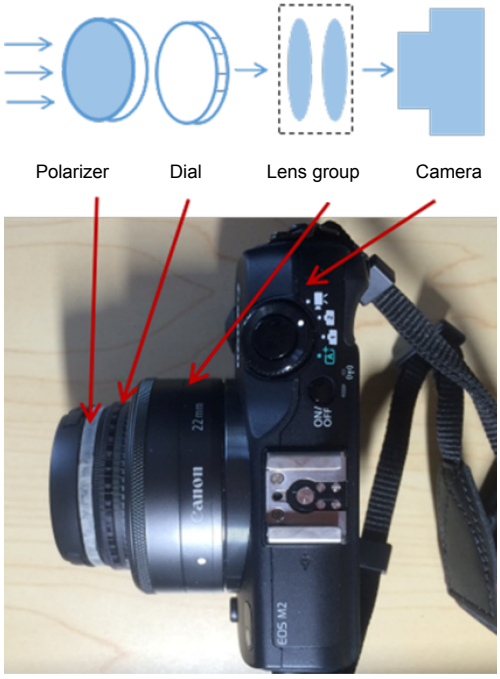

Fig. 2 Photograph and configuration of the polarized camera device

We measure the residue polarization of the CCD using an integrating sphere (Thorlabs, IS200) as the non-polarized light source and a rotating polarizer to generate linearly polarized light of constant intensity and varying angles. Residue polarization values for all the pixels are less than 3%. This effect is ignored in the data analysis.

For polarization imaging, we rotate the polarizer in front of the camera lens (PSA) and take three pictures corresponding to 0°, 45°, and 90° polarization directions. The linear part of the polarization states or the Stokes vector components (S_i, i=0, 1, 2) can be expressed as (He et al., 2015)

$$\begin{cases} S_0 = I(0°) + I(90°), \\ S_1 = I(0°) - I(90°), \\ S_2 = 2I(45°) - I(0°) - I(90°). \end{cases} \tag{1}$$

The degree of linear polarization (DoLP) and angle of polarization (AoP) can be obtained from the Stokes vectors, expressed as

$$\mathrm{DoLP}=\frac{\sqrt{S_1^2+S_2^2}}{S_0}, \tag{2}$$

$$\mathrm{AoP}=\frac{1}{2}\arctan(S_2/S_1). \tag{3}$$

3 Experimental results

3.1 Grazing incidence unpolarized illumination and unpolarized imaging

Using the experimental setup shown in Fig. 1, illuminating the footwear prints with wide-field footwear print search light, and imaging the footwear prints with unpolarized light, we obtain the light intensity pictures corresponding to the three-color channels. Fig. 3a shows the image of the blue channel. It shows that grazing incidence illumination helps obtain footwear prints on the PVC floor cover, but the image contrast is not high.

3.2 Grazing incidence polarized illumination and unpolarized imaging

We add a linear polarizer in front of the footwear print search light and take intensity images without the PSA. Fig. 3b shows the footwear print intensity image under linearly polarized illumination with the polarization direction parallel to the ground. Images with the direction of linear polarization perpendicular to the ground are tested, but the results are not shown since the footwear print image does not show up clearly. The comparison between Figs. 3a and 3b shows that polarized grazing incidence illumination improves the footwear print contrast.

3.3 Grazing incidence polarized illumination and polarized imaging

We take the footwear print intensity images with the polarized grazing incidence illumination and polarized imaging. Three linear polarization images are obtained corresponding to the three rotation angles of the PSA, i.e., 0°, 45°, and 90° to the direction of illumination polarization. Fig. 3c shows the polarization component images with 0° analyzer, which has the highest contrast among the three images. Since the particles on the footwear print are mainly Rayleigh scatterers, 0° polarization dominates the scattered light if measured at 90° (scattering angle) to the incident direction, leading to the highest contrast in 0° PSA. Fig. 3c shows that images of the parallel linear polarization component results in further improvement in the contrast of footwear print images.

Using the three linear polarization component images and Eqs. (1)–(3), we can further calculate the DoLP image (Fig. 3d). It is apparent that the DoLP can effectively reduce the background and significantly improve the contrast of the footprint image. We calculate the AoP image, but do not show the results because the contrast is much lower.

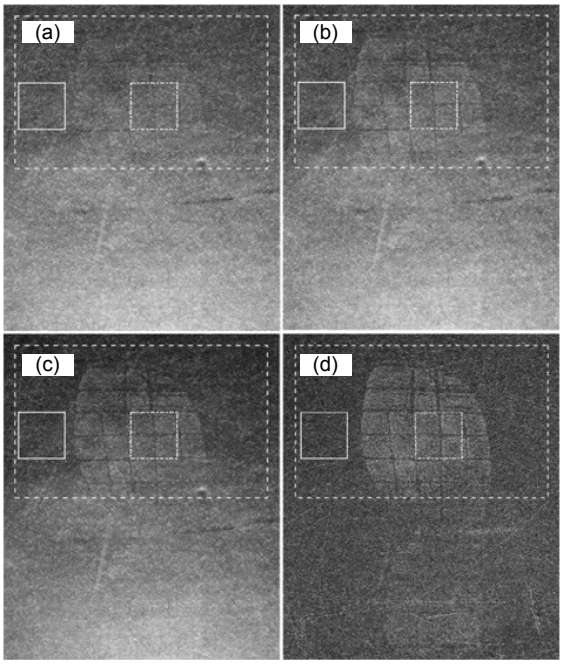

Fig. 3 Footwear print images in different experimental conditions: (a) image with unpolarized illumination and unpolarized imaging; (b) image with polarized illumination and unpolarized imaging; (c) image with polarized illumination and polarized imaging; (d) DoLP image

4 Quantitative data analysis

We conduct quantitative analysis on footwear print images. We choose the frontal part of a footwear print since it is usually clearer and carries more forensic information on individual characteristics (Winkelmann, 1987). We select a square in this part of the footwear print image and another square of equal area in the image of PVC floor cover (ground) for quantitative data analysis (Fig. 3).

We calculate the histograms of the selected

image areas (large dashed box) with and without the footwear print in Fig. 3 and display the histogram curves in Fig. 4. $I_{UU\text{-}F}$ and $I_{UU\text{-}G}$ represent the intensity values of the footwear prints and the ground in the unpolarized illumination and unpolarized imaging condition, respectively; $I_{PU\text{-}F}$ and $I_{PU\text{-}G}$ represent the intensity values of the footwear prints and the ground in the polarized illumination and unpolarized imaging condition, respectively; $I_{PP\text{-}F}$ and $I_{PP\text{-}G}$ represent the intensity values of the footwear prints and the ground in the polarized illumination and polarized imaging condition, respectively; DoLP_F and DoLP_G represent the DoLP values of the footwear prints and the ground in the polarized illumination and polarized imaging condition, respectively. Each pixel depth is 16. A detailed examination of the footwear print images in Fig. 3 and their corresponding histogram curves in Fig. 4 helps learn how the contrasts vary in different measurements. For unpolarized imaging, changing the illumination from unpolarized to polarized light does not affect the image of the ground. Contrast enhancement is achieved by slight increase in the scattering intensity of the footwear print. For detection of the parallel linear polarization component, the increase of contrast is due to the reduction of background in images of the footwear print and the ground. In the DoLP image, the decrease in the footwear print and the ground is even larger, resulting in significant enhancement in contrast.

To quantitatively examine the experimental results, we calculate the contrast ratios between the footwear print (small dashed square in Fig. 3) and the ground (small solid square in Fig. 3) under different imaging conditions. We take the red, green, and blue channel data and calculate the contrasts corresponding to different wavelengths. Results are listed in Table 1. Contrasts are calculated using the following definition:

$$C=\frac{a-b}{a+b}, \tag{4}$$

where a and b represent the intensity mean values of the footwear print and the ground, respectively. $C_{I\text{-}UU}$ represents the intensity contrast value of the footwear print and the ground in the unpolarized illumination and unpolarized imaging condition; $C_{I\text{-}PU}$ represents the intensity contrast value of the footwear print and the ground in the polarized illumination and unpolarized imaging condition; $C_{I\text{-}PP}$ represents the intensity contrast value of the footwear print and the ground in the polarized illumination and polarized imaging condition; C_{DoLP} represents the contrast value of degree of linear polarization.

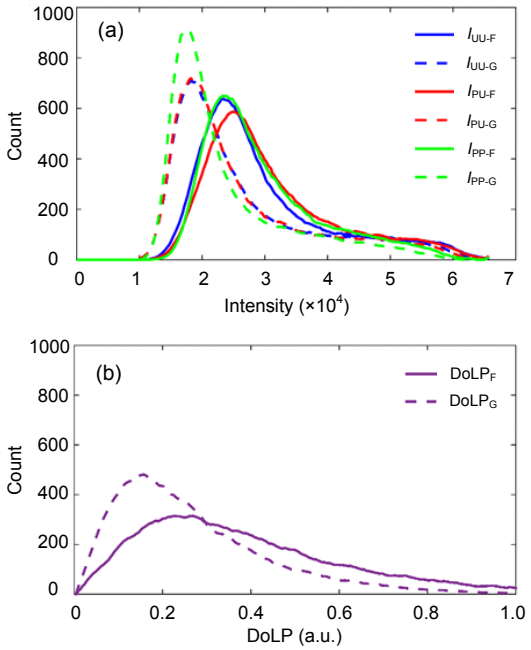

Fig. 4 Histogram curves corresponding to the intensity (a) and the DoLP (b) of footwear prints

Table 1 Contrast ratios of different background materials

Background	Color channel	$C_{I\text{-}UU}$	$C_{I\text{-}PU}$	$C_{I\text{-}PP}$	C_{DoLP}
PVC floor	Red	0.06	0.09	0.11	0.17
	Green	0.06	0.08	0.10	0.18
	Blue	0.06	0.09	0.10	0.20
Tile 1	Red	0.04	0.10	0.11	0.19
	Green	0.04	0.10	0.11	0.19
	Blue	0.07	0.15	0.17	0.19
Tile 2	Red	0.02	0.06	0.07	0.20
	Green	0.02	0.06	0.07	0.21
	Blue	0.02	0.07	0.08	0.23

We carry out similar experiments on footwear prints left on two types of household tiles (Figs. 1c and 1d). These tiles are made of ceramic materials with rough surfaces for anti-slippery effects. Surface morphologies of these tiles and the PVC floor are similar. Table 1 shows that the experimental data for

the footwear prints on these tiles is quite similar to that on the PVC floor. Contrast ratios increase from $C_{\text{I-UU}}$ to C_{DoLP}, and the blue channel achieves the highest contrast ratio.

In summary, experimental results clearly demonstrate that linearly polarized illumination and detection helps enhance the contrast of images. For DoLP images, using smaller wavelengths will result in even higher contrast.

In fact, the spectral property for the contrast of DoLP images depends on many parameters of the scattering particles on the footwear prints and the surface of the ground. The refractive indices, sizes, and shapes of particles, as well as the surface morphology of the ground, may all affect the contrast at different wavelengths.

5 Simulation and analysis of polarized light scattering

The footwear prints actually represent disturbances to the surface conditions, such as changes in the density of particles by pressure or exogenous particles of different sizes and optical properties. For unpolarized light, the scattered light intensity is sensitive mainly to the size, density, and relative refractive index of the scattering particles. For polarized light, however, the intensity and polarization states of the scattered light are sensitive to not only the size, density, and relative refractive index of the particles, but also many other properties, such as shape, orientation and alignment, surface morphology, and birefringence. Compared with unpolarized light, polarized light scattering can provide much richer information to differentiate different surfaces, all of which may be explored to increase the contrast in footwear print images.

For better understanding the physical mechanisms for contrast enhancement of footwear prints by polarized grazing incidence and polarized scattering detection, we use a very crude scattering model and a Monte Carlo simulation program (Yun et al., 2009; del Moral, 2013) to demonstrate how the intensity and polarization states of the scattered light vary for different samples and experimental configurations. This program simulates photon transport in multilayered turbid media. A brief summary of the model is as follows: A collection of spherical particles with normally distributed sizes are assumed to mimic the polarized light scattering properties of the footwear prints and the ground. For the footwear prints, particle sizes are centered in 1 μm and cover the sub-micron region; for the ground, we assume the sphere diameter centered in 10 μm. Both types of particles are in air, the refractive indices are set to 1.54 (Weinzierl et al., 2009), the scattering coefficients of the two types of particles are 200 cm^{-1}, and the illumination wavelength is set to 467 nm. Fig. 5 shows the simulated contrasts. The simulation results follow the trend of the experimental results on the PVC floor cover, both of which indicate that polarization incidence and detection enhance the contrast. The relatively small size or the probable sharp edges of the extraneous particles on the footwear prints may play a vital role in the contrast enhancement of the polarization images.

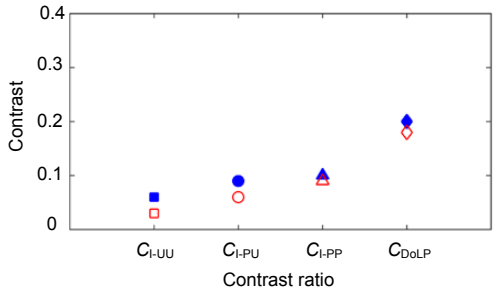

Fig. 5 Experimental and simulated contrast ratios under different imaging conditions at 467-nm wavelength incident light
Solid dots represent experimental values on the PVC floor cover, and hollow dots represent simulation values

6 Conclusions

We have carried out grazing incident polarization imaging of footwear prints using commercial wide-field footwear print search light and a color digital camera. The current work provides us a useful method to obtain the footwear prints of criminals, which is of great significance in detecting cases. By placing linear polarizers in front of light and camera lens, we have tested different experimental configurations for footwear print images. Results showed that illumination by linearly polarized light with the polarization direction parallel to the ground will improve the image contrast for even unpolarized

detection. Further enhancement of the contrast has been achieved by detection of the linearly polarized component parallel to the incident beam polarization. Furthermore, data processing showed that significant improvement is achieved for degree of linear polarization (DoLP) imaging, but not for angle of polarization (AoP) imaging. The deployment of a three-color camera helps enhance grazing incidence polarized light imaging by providing the spectral features of footwear prints. For the blue, green, and red color channels, DoLP contrast increases for smaller wavelengths.

Acknowledgements

The authors thank Dr. Dong-sheng CHEN from Department of Physics, Tsinghua University for providing the simulation tools.

Compliance with ethics guidelines

Xin-yi BI, Rui-fang HAN, Ran LIAO, Wu-sheng FENG, Da LI, Xue-jie ZHANG, and Hui MA declare that they have no conflict of interest.

References

Anderson K, Gaston KJ, 2013. Lightweight unmanned aerial vehicles will revolutionize spatial ecology. *Front Ecol Environ*, 11(3):138-146. https://doi.org/10.1890/120150

Bennett MR, Huddart D, Gonzalez S, 2009. Preservation and analysis of three-dimensional footwear evidence in soils: the application of optical laser scanning. In: Ritz K, Dawson L, Miller D (Eds.), Criminal and Environmental Soil Forensics. Springer, Dordrecht, p.445. https://doi.org/10.1007/978-1-4020-9204-6_28

Bodziak WJ, 1999. Footwear Impression Evidence: Detection, Recovery and Examination (2nd Ed.). CRC Press, Florida, USA.

Bohren CF, Huffman DR, 1983. Absorption and Scattering of Light by Small Particles. Wiley, New York, USA.

Cai FH, Lu W, Shi WX, et al., 2017. A mobile device-based imaging spectrometer for environmental monitoring by attaching a lightweight small module to a commercial digital camera. *Sci Rep*, 7:15602. https://doi.org/10.1038/s41598-017-15848-x

del Moral P, 2013. Mean Field Simulation for Monte Carlo Integration. CRC Press, Florida, USA.

Ghosh N, Vitkin IA, 2011. Tissue polarimetry: concepts, challenges, applications, and outlook. *J Biomed Opt*, 16(11), Article 110801. https://doi.org/10.1117/1.3652896

He C, Chang JT, Wang Y, et al., 2015. Linear polarization optimized Stokes polarimeter based on four-quadrant detector. *Appl Opt*, 54(14):4458-4463. https://doi.org/10.1364/AO.54.004458

Herod DW, Menzel ER, 1982. Laser detection of latent fingerprints: ninhydrin followed by zinc chloride. *J Forens Sci*, 27(3):513-518.

Krishan K, 2007. Individualizing characteristics of footprints in Gujjars of North India—forensic aspects. *Forens Sci Int*, 169(2-3):137-144. https://doi.org/10.1016/j.forsciint.2006.08.006

Li KW, Yu RF, Zhang W, 2011. Roughness and slipperiness of floor surface: tactile sensation and perception. *Saf Sci*, 49(3):508-512. https://doi.org/10.1016/j.ssci.2010.11.010

Li XP, Liao R, Ma H, et al, 2018. Polarimetric learning: a Siamese approach to learning distance metrics of algal Mueller matrix images. *Appl Opt*, 57(14):3829-3837. https://doi.org/10.1364/AO.57.003829

Li ZW, Wei CH, Li Y, et al., 2011. Research of shoeprint image stream retrieval algorithm with scale-invariance feature transform. Proc Int Conf on Multimedia Technology, p.5488-5491. https://doi.org/10.1109/ICMT.2011.6002147

Liou KN, Takano Y, Yang P, 2013. Intensity and polarization of dust aerosols over polarized anisotropic surfaces. *J Quant Spectrosc Radiat Transf*, 127:149-157. https://doi.org/10.1016/j.jqsrt.2013.05.010

Migliavacca M, Galvagno M, Cremonese E, et al, 2011. Using digital repeat photography and eddy covariance data to model grassland phenology and photosynthetic CO_2 uptake. *Agric Forest Meteor*, 151(10):1325-1337. https://doi.org/10.1016/j.agrformet.2011.05.012

Mora M, Sbarbaro D, 2005. A robust footprint detection using color images and neural networks. Iberoamerican Congress on Pattern Recognition, p.311-318. https://doi.org/10.1007/11578079_33

Nakajima K, Mizukami Y, Tanaka K, et al., 2000. Footprint-based personal recognition. *IEEE Trans Biomed Eng*, 47(11):1534-1537. https://doi.org/10.1109/10.880106

Namer E, Shwartz S, Schechner YY, 2009. Skyless polarimetric calibration and visibility enhancement. *Opt Expr*, 17(2):472-493. https://doi.org/10.1364/OE.17.000472

Renaud G, Lazzari R, Leroy F, 2009. Probing surface and interface morphology with grazing incidence small angle X-ray scattering. *Surf Sci Rep*, 64(8):255-380. https://doi.org/10.1016/j.surfrep.2009.07.002

Shaler RC, 2011. Crime Scene Forensics: a Scientific Method Approach. CRC Press, Florida, USA.

Sheets HD, Gross S, Langenburg G, et al., 2013. Shape measurement tools in footwear analysis: a statistical investigation of accidental characteristics over time. *Forens Sci Int*, 232(1-3):84-91. https://doi.org/10.1016/j.forsciint.2013.07.010

Shin D, Pierce MC, Gillenwater AM, et al., 2010. A fiber-optic fluorescence microscope using a consumer-grade digital camera for in vivo cellular imaging. *PLOS ONE*, 5(6), Article e11218.

https://doi.org/10.1371/journal.pone.0011218

Snik F, Craven-Jones J, Escuti M, et al., 2014. An overview of polarimetric sensing techniques and technology with applications to different research fields. SPIE, p.1-20. https://doi.org/10.1117/12.2053245

Svensen Ø, Stamnes JJ, Kildemo M, et al., 2011. Mueller matrix measurements of algae with different shape and size distributions. *Appl Opt*, 50(26):5149-5157. https://doi.org/10.1364/AO.50.005149

Tuchin VV, 2016. Polarized light interaction with tissues. *J Biomed Opt*, 21(7):0711147. https://doi.org/10.1117/1.JBO.21.7.071114

Tyo JS, Goldstein DL, Chenault DB, et al., 2006. Review of passive imaging polarimetry for remote sensing applications. *Appl Opt*, 45(22):5453-5469. https://doi.org/10.1364/AO.45.005453

Wagle MSUY, 2015. Footwear Impression Analysis: Implementing a Model for Automatic Shoeprint Recognition to Use in Forensic Science. MD Thesis, Blekinge Institute of Technology, Blekinge, Sweden.

Wang Y, He HH, Chang JT, et al., 2016. Mueller matrix microscope: a quantitative tool to facilitate detections and fibrosis scorings of liver cirrhosis and cancer tissues. *J Biomed Opt*, 21(7):0711127. https://doi.org/10.1117/1.JBO.21.7.071112

Wang Y, Liao R, Dai J, et al., 2018. Differentiation of suspended particles by polarized light scattering at 120°. *Opt Expr*, 26(17):22419-22431. https://doi.org/10.1364/OE.26.022419

Webster JG, 1998. The Measurement, Instrumentation and Sensors Handbook. CRC Press, Florida, USA.

Weinzierl B, Petzold A, Esselborn M, et al., 2009. Airborne measurements of dust layer properties, particle size distribution and mixing state of Saharan dust during SAMUM 2006. *Tellus B Chem Phys Meteorol*, 61(1):96-117. https://doi.org/10.1111/j.1600-0889.2008.00392.x

Winkelmann W, 1987. Use of footprints, especially forefoot prints, from the forensic viewpoint. *Z Rechtsmed*, 99(2):121-128.

Wolff LB, 1997. Polarization vision: a new sensory approach to image understanding. *Image Vis Comput*, 15(2):81-93. https://doi.org/10.1016/S0262-8856(96)01123-7

York T, Powell SB, Gao S, et al., 2014. Bioinspired polarization imaging sensors: from circuits and optics to signal processing algorithms and biomedical applications. *Proc IEEE*, 102(10):1450-1469. https://doi.org/10.1109/JPROC.2014.2342537

Yun TL, Zeng N, Li W, et al., 2009. Monte Carlo simulation of polarized photon scattering in anisotropic media. *Opt Expr*, 17(19):16590-16602. https://doi.org/10.1364/OE.17.016590

Zinov'eva TV, 2008. Investigation of the linear polarization in infrared absorption bands. *Astron Lett*, 34(2):118-132. https://doi.org/10.1134/S1063773708020059